Fragile protein folds: Sequence and environmental factors affecting the equilibrium of two interconverting, stably folded protein conformations

Xingjian Xu[1,2], Igor Dikiy[1,3], Matthew R. Evans[4], Leandro P. Marcelino[1,5], Kevin H. Gardner[1,5,6]

[1]Structural Biology Initiative, CUNY Advanced Science Research Center, New York, NY, USA

[2]Ph.D. Program in Biochemistry, The Graduate Center, CUNY, New York, NY, USA

[3]Current address: Regeneron Pharmaceuticals, Tarrytown, NY, USA

[4]Current address: Acclaim Physician Group, Inc. Fort Worth, TX, USA

[5]Department of Chemistry and Biochemistry, City College of New York, New York, NY, USA

[6]Biochemistry, Chemistry and Biology Ph.D. Programs, The Graduate Center, CUNY, New York, NY, USA

Correspondence: Kevin Gardner (kgardner@gc.cuny.edu)

Abstract. Recent research on fold-switching metamorphic proteins has revealed some notable exceptions to Anfinsen's hypothesis of protein folding. We have previously described how a single point mutation can enable a well-folded protein domain, one of the two PAS (Per-ARNT-Sim) domains of the human ARNT (aryl hydrocarbon receptor nuclear translocator) protein, to interconvert between two conformers related by a slip of an internal β-strand. Using this protein as a test case, we advance the concept of a "fragile fold," a protein fold that can reversibly rearrange into another fold that differs by a substantial number of hydrogen bonds, entailing reorganization of single secondary structure elements to more drastic changes seen in metamorphic proteins. Here we use a battery of biophysical tests to examine several factors affecting the equilibrium between the two conformations of the switching ARNT PAS-B Y456T protein. Of note, we find that factors which impact the HI loop preceding the shifted Iβ-strand affect both the equilibrium levels of the two conformers and the denatured state which links them in the interconversion process. Finally, we describe small molecules that selectively bind to and stabilize the wildtype conformation of ARNT PAS-B. These studies form a toolkit for studying fragile protein folds and could enable ways to modulate the biological functions of such fragile folds, both in natural and engineered proteins.

MAGNETIC RESONANCE
Open Access
Discussions

1   Introduction

Anfinsen's hypothesis, which states that a protein's primary sequence encodes a unique fold or conformation, has
30   dominated the study of protein folding for almost 50 years (Anfinsen, 1973). However, it is increasingly clear that a range of
exceptions to the "one sequence, one fold" concept are widely found in biology. One counterexample is the intrinsic
disorder found in a significant number of functional proteins and protein regions. These intrinsically-disordered regions do
not adopt a stable three-dimensional structure, instead existing as conformational ensembles of states that may include pre-
formed structural nuclei (Dyson, 2016). Other counterexamples are provided by proteins which interconvert among multiple
35   folded states, ranging from a "fragile fold", in which substitution of a few amino acids – even one – results in the domain co-
existing in two states (Evans et al., 2009;Evans and Gardner, 2009;Ha and Loh, 2012), to the general concept of a
"metamorphic protein," one that can reversibly adopt different stable folds in different environmental conditions (Murzin,
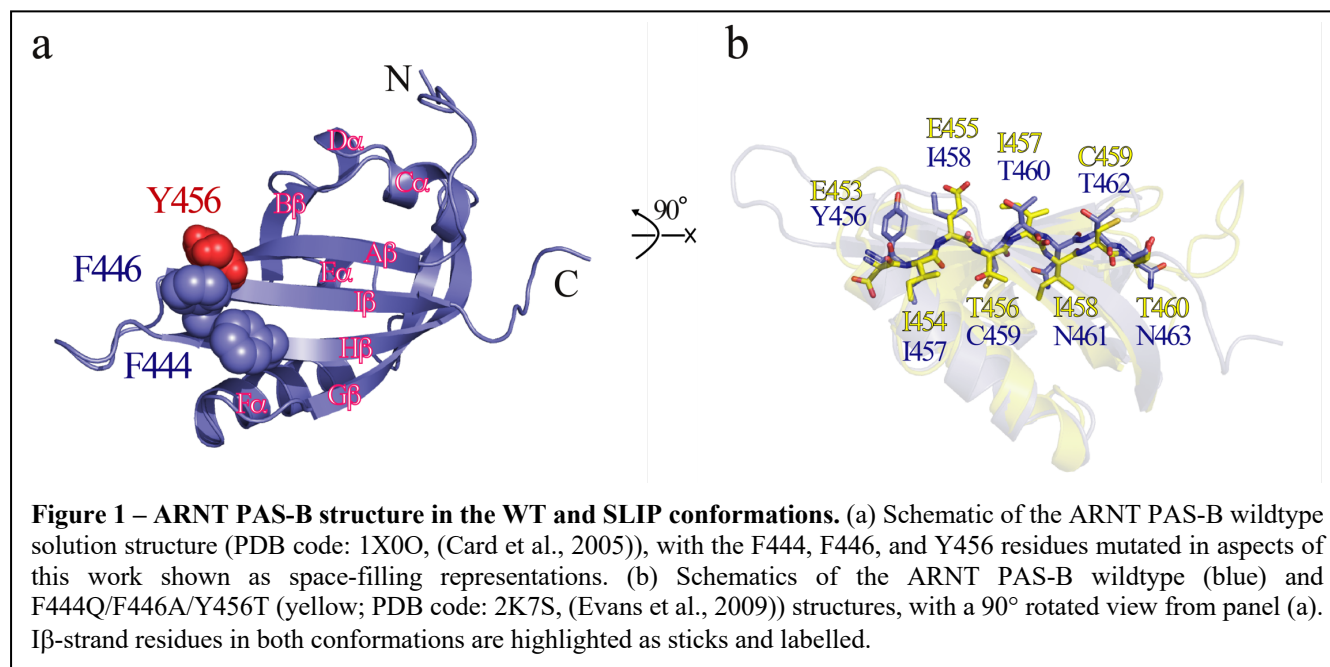2008).

We consider a protein or domain to have a "fragile fold" if it can populate two stable folds and interconvert
40   reversibly between them, doing so via breaking and reforming a substantial number of hydrogen bonds. This concept differs
from that of simple protein conformational switches (Gerstein and Echols, 2004) mainly in the extent of hydrogen bond
network remodeling. For example, we previously reported the Y456T mutant of PAS-B (Per-ARNT-Sim) domain of the
human ARNT (Aryl hydrocarbon Receptor Nuclear Translocator) protein, which undergoes a 3-residue β-strand slip
requiring 15 of the 26 inter-strand hydrogen bonds in the β-sheet to be broken and re-formed while still retaining the same
45   overall topology (Evans et al., 2009;Evans and Gardner, 2009). In metamorphic proteins, which can be considered an
extreme case of a fragile fold, an even greater number of hydrogen bonds differ between the two folds as seen in
lymphotactin (which alternates between a conventional chemokine fold and a dimeric β-sandwich (Kuloğlu et al.,
2002;Tuinstra et al., 2008)). These studies suggest that protein folds may hide unforeseen flexibility or fragility which can be
trivially accessed by small changes in sequence or environmental conditions, facilitating the evolution of new folds and
50   protein domains (Yadid et al., 2010;Tuinstra et al., 2008;Alexander et al., 2009).

To experimentally probe such fragile folds, we here use the abovementioned ARNT PAS-B Y456T point mutant as
a model system. ARNT is a eukaryotic bHLH-PAS transcription factor that dimerizes with other bHLH-PAS proteins (e.g.
AhR, HIF-α) to bind DNA and regulate gene expression in response to a varied set of stimuli (Labrecque et al., 2013). In
addition to the bHLH (basic-helix-loop-helix) DNA binding module and C-terminal coactivator domains, these proteins
55   contain two PAS (Per-ARNT-Sim) domains (PAS-A and PAS-B), which are essential for heterodimerization (Erbel et al.,
2003;Chapman-Smith et al., 2004;Wu et al., 2015). The typical PAS domain fold is 100-120 residues in length and consists
of several α-helices packed against one side of a five-stranded, anti-parallel β-sheet, often enclosing a ligand-binding cavity
(Card et al., 2005;Wu et al., 2015;Wu et al., 2019;Bisson et al., 2009), **Figure 1a**. PAS domains provide binding sites for
many diverse binding partners, including other PAS domains (Cardoso et al., 2012;Erbel et al., 2003;Huang et al.,
60   2012;Scheuermann et al., 2009;Wu et al., 2015), adjacent helices (Harper et al., 2003;Nash et al., 2011;Rivera-Cancel et al.,

MAGNETIC RESONANCE Discussions

2014), and coiled-coil coactivators (Guo et al., 2013;Guo et al., 2015). Notably, changes in the occupancy or configuration of bound small molecule ligands can modulate the protein/protein interactions of many PAS domains (Scheuermann et al., 2009), opening the door to natural and artificial control of signaling pathways.

65 While designing point mutants to disrupt the interactions between the ARNT PAS-B domain and other binding partners, we fortuitously discovered that the Y456T variant existed in a slow conformational equilibrium between two equally-populated conformations (Evans et al., 2009). Solution NMR studies revealed that the new conformation primarily differs from the native fold by a +3 slip in register and accompanying inversion of the central Iβ-strand (**Figure 1b**); hence, we termed the conformations "WT" and "SLIP." Interestingly, the SLIP conformation does not bind HIF-2α PAS-B (Evans et al., 2009), consistent with the involvement of the ARNT PAS-B beta sheet in this interaction (Scheuermann et al.,

70 2009;Wu et al., 2015). With a combination of solution NMR approaches, spanning real-time NMR (Evans and Gardner, 2009) to high-pressure perturbation of the equilibrium (Xu, 2020), we have discovered that the interconversion between WT and SLIP conformations likely requires global unfolding, as might be expected from the large number of hydrogen bonds disrupted by the conformational slip.

Figure 1 – ARNT PAS-B structure in the WT and SLIP conformations. (a) Schematic of the ARNT PAS-B wildtype solution structure (PDB code: 1X0O, (Card et al., 2005)), with the F444, F446, and Y456 residues mutated in aspects of this work shown as space-filling representations. (b) Schematics of the ARNT PAS-B wildtype (blue) and F444Q/F446A/Y456T (yellow; PDB code: 2K7S, (Evans et al., 2009)) structures, with a 90° rotated view from panel (a). Iβ-strand residues in both conformations are highlighted as sticks and labelled.

Here we more broadly examine other factors that determine the equilibrium populations of these two folds, with

75 interest in both characterizing these effects and artificially manipulating the interconversion as a possible route to engineering novel switchable proteins. We start by characterizing the temperature dependence of the interconversion process, allowing us to extract thermodynamic parameters of it. We also show that several features of the HI loop region, which precedes the shifting Iβ strand, can also influence the WT:SLIP ratio. In addition, we demonstrate mutations in this region and the Hβ-strand proceeding the HI loop can also affect the denatured state of the protein, resulting in differential

80 refolding to one of the two conformations during interconversion. Lastly, we identify compounds that can preferentially bind one conformer over another, giving us the ability to shift the relative populations between these two conformations. Many of the approaches discussed here exemplify ways of studying and manipulating other fragile folds or metamorphic proteins, both in natural and engineered contexts as ligand-regulated sensors and switches (Ha and Loh, 2017).

2 Materials and Methods

85 ### 2.1 Cloning, expression, and purification of ARNT PAS-B mutants

Plasmid DNA encoding the human ARNT PAS-B domain [residues 356-470] was used to introduce various point mutations, using the QuikChange Site-Directed Mutagenesis Kit (Stratagene). Following PCR amplification and digestion of the parental template with DpnI, using the manufacturers' instructions, the modified plasmid was transformed into the pHis-parallel bacterial expression vector (Sheffield et al., 1999). The accuracy of each mutation was verified by sequencing.

90 ARNT PAS-B mutant constructs were transformed into *E. coli* BL21 (DE3) cells. For isotopically-labelled protein expression, cultures were grown in M9 minimal media containing 1 g/L $^{15}NH_4Cl$ for uniformly ^{15}N-labeled samples or 1 g/L $^{15}NH_4Cl$ and 3 g/L ^{13}C glucose for uniformly $^{13}C,^{15}N$-labeled samples, at 37 °C. Once the cell density (A_{600}) measured 0.6-0.8, protein expression was induced with 0.5 mM isopropyl β-D-thiogalactoside. Following 15 hr at 20 °C, cell pellets were harvested and resuspended in 20 mL of 50 mM Tris (pH 7.5), 15 mM NaCl and 20 mM imidazole. Cells were lysed by high-

95 pressure extrusion, centrifuged, and filtered using a 0.45 μm pore size filter. The supernatant was loaded over a Ni^{2+}-NTA affinity column and eluted using a linear 20-500 mM imidazole gradient. The resulting sample was exchanged into an imidazole-free buffer (50 mM Tris [pH 7.5], 15 mM NaCl) and incubated overnight in the presence of His_6-TEV protease. Following His_6-tag cleavage, the remaining protein was purified away from free His_6-tag and His_6-TEV with an additional pass over a Ni^{2+}-NTA column and concentrated in an Amicon pressure-driven ultrafiltration cell with YM-10 10 kDa filters.

100 The resulting protein contains a four-residue vector-derived N-terminal cloning artifact, GAMD, plus residues 356-470 of ARNT PAS-B.

2.2 NMR analysis of ARNT PAS-B Y456T equilibrium constant

Solution NMR studies of ARNT PAS-B and its mutants were conducted in 50 mM Tris, 17 mM NaCl and 5 mM DTT. To determine the effects that buffer and pH have on the stability of each conformation, ARNT PAS-B Y456T was

105 exchanged into either 50 mM Tris (pH range 7-9) or PIPES (pH range 6-7.5), 17 mM NaCl, and 5 mM DTT. ^{15}N-^1H HSQC spectra of 200 μM protein were recorded more than 20 hr post-exchange to allow adequate time for any perturbations to the conformational equilibrium to be established. To determine the effects of temperature on the equilibrium constant, ^{15}N-^1H HSQC spectra of 200 μM ARNT PAS-B Y456T in 50 mM Tris, 17 mM NaCl and 5 mM DTT were recorded after incubation for a sufficient time (2-4 hr) to ensure equilibrium was established at temperatures between 278 K and 328 K in

110 5 K increments. All NMR spectra were processed using NMRpipe (Delaglio et al., 1995) and NMRFx (Johnson, 2018;Norris et al., 2016) and analyzed using NMRViewJ (Johnson and Blevins, 1994;Johnson, 2018). We measured the WT:SLIP conformational equilibrium as the relative volume of several well-dispersed peaks originating from each conformation.

2.3   NMR analysis of unfolded state of ARNT PAS-B mutants

We populated the unfolded state of wildtype, Y456T, and F444Q/F446A/Y456T mutant ARNT PAS-B by
115 denaturing these proteins in 8 M urea. HNCO, HN(CA)CO, HNCACB, and CBCA(CO)NH spectra were collected at 25 °C on 500 μM uniformly $^{13}C,^{15}N$-labeled protein in 8 M urea, 50 mM Tris pH 7.5, 20 mM NaCl, 5 mM beta-mercaptoethanol and used to assign ~95% of the HN, N, C', Cα, and Cβ resonances. We then used HN, N, Cα, and Cβ chemical shifts from the CBCA(CO)NH experiment to predict S^2 order parameters using the TALOS+ program (Shen et al., 2009) and the Cα and Cβ chemical shifts to predict residual secondary structure using the SSP program (Marsh et al., 2006).

120 ### 2.4   Ligand screening by thermal shift assay and NMR

The ligand screen was conducted against ARNT PAS-B wildtype, Y456T, and F444Q/Y456T proteins using the thermal shift assay (Pantoliano et al., 2001). Each well of a 384-well plate was loaded with 1 μM protein, 50 μM compound, and 1X Sypro Orange dye and brought to a final volume of 100 μL in 50 mM Tris (pH 7.5), 17 mM NaCl and 2.5% DMSO. All experiments were conducted in duplicate. Using an Applied Biosystems 7500 Real-Time PCR machine and excitation
125 and fluorescence emission wavelengths for Sypro Orange (λ_{ex} = 475 nm, λ_{em} = 590 nm), we recorded fluorescence intensities in 1 ºC increments between 25 ºC and 95 ºC, with a time delay of thirty seconds between data points to ensure the samples were at the proper temperature. Due to the extremely slow interconversion rate between the two conformations of ARNT PAS-B Y456T, here we presume the conformational equilibrium between the two states of this mutant to be constant. Using a Boltzmann sigmoidal curve with a 95% confidence band, the T_m for each well was determined. We considered ligand-
130 induced shifts in T_m of 4 ºC or greater as indicative of a potential binder. Of note, we used ARNT PAS-B F444Q/Y456T (WT:SLIP; 19:81) to establish ligand binding to ARNT PAS-B predominantly in the SLIP conformation instead of ARNT PAS-B F444Q/F446A/Y456T (WT:SLIP; 1:99), since the high stability of the triple mutant made it difficult to record the full transition needed for an accurate calculation of T_m.

We used solution NMR to establish which protein residues were interacting with the compounds identified by the
135 thermal shift assay. Purified protein samples of wildtype, Y456T, or F444Q/F446A/Y456T ARNT PAS-B protein at 180 μM were combined with a single compound at a final concentration of 220 μM and a ^{15}N-^1H HSQC spectrum was recorded. Samples remained at room temperature for 24 hours before recording the spectrum to ensure equilibrium had been reached. We considered either chemical shift or peak intensity changes as confirmation of ligand binding.

2.5 KG-548 and KG-655 binding titration analysis

140 To determine the binding affinity for compound KG-548, we conducted a ^{15}N-^{1}H HSQC titration series with increasing concentrations of KG-548 (0, 25, 50, 100, 200, 500, and 1000 μM) against a constant 200 μM concentration of ARNT PAS-B Y456T. ^{15}N-^{1}H HSQC spectra were recorded 24 hr after samples were mixed to allow sufficient time to reach equilibrium. The concentration of ligand-bound WT conformation ($C_{WT,B}$) was derived from peak intensities, plotted versus the ligand concentration (C_L), and fit to the following equation to derive dissociation constant (K_d) and maximal binding

145 (B_{max}):

$$C_{WT,B} = B_{max} * C_L / (K_d + C_L) \qquad (1)$$

We attempted to determine the concentration of ligand-bound protein directly from peak intensities; however, this analysis was complicated by the broadening of WT peaks in the presence of KG-548. In order to overcome this challenge, we used the following protocol to determine the concentration of ligand-bound WT conformation.

150 We measured peak volumes for those peaks that showed no chemical shift changes, which report on both bound and unbound states of the protein. The relative peak volumes of the peaks corresponding to each conformation indicate the relative concentrations of total WT and SLIP conformations, but not the ligand-bound and ligand-free concentrations. We calculated the concentration of the SLIP conformation (C_{+3}), which does not bind compound appreciably, and the total concentration of WT conformation ($C_{WT,T}$) at each concentration of compound, by comparing these peak volumes (V_{WT}, V_{+3})

155 to those in the absence of compound:

$$C_{WT,T} = C_{WT,0} * (V_{WT}/V_{WT,0}) \qquad (2)$$
$$C_{+3} = C_{+3,0} * (V_{+3}/V_{+3,0}) \qquad (3)$$

Then, assuming that the SLIP conformation remains in the same equilibrium with the unbound WT conformation as in the absence of compound, we estimated the concentration of ligand-bound WT conformation as:

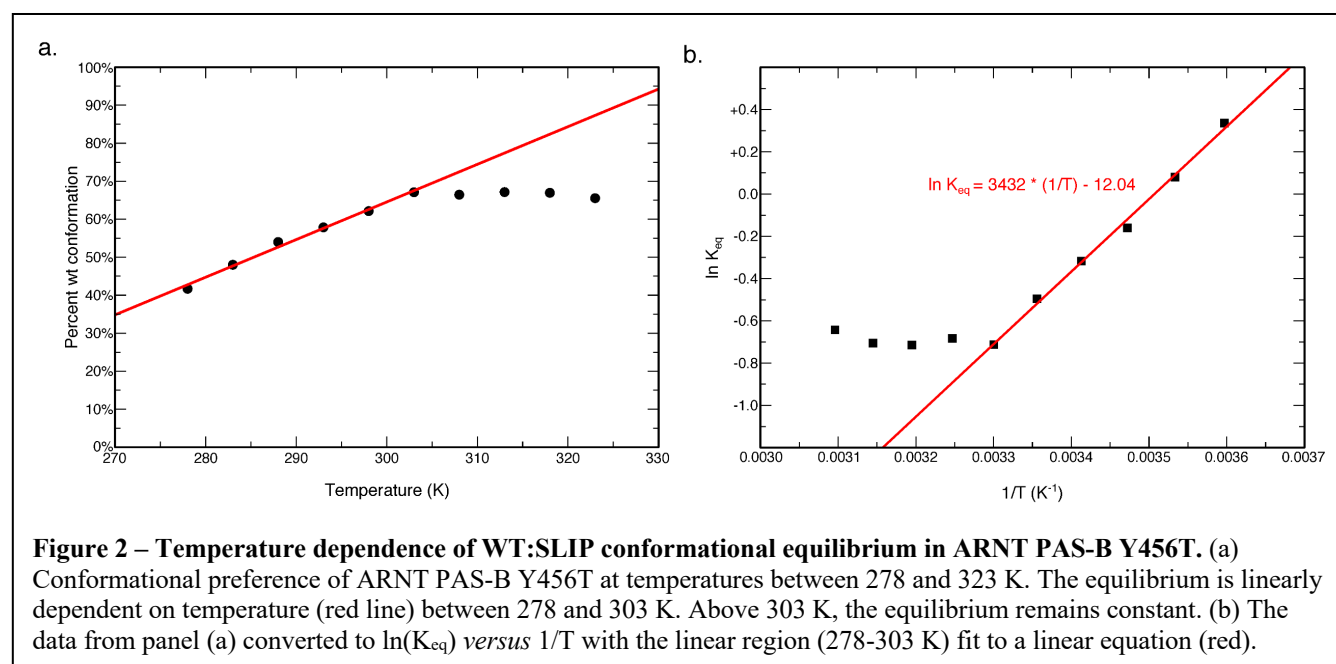160 $$C_{WT,B} = C_{WT,T} - C_{+3} \qquad (4)$$

Most of the residues used in the titration analysis for KG-548 showed chemical shift changes and peak broadening in the presence of KG-655, rendering them unusable for the method described above. We therefore conducted ^{13}C-^{1}H HSQC titration experiments instead. We monitored the L391 δ1 methyl peaks which are particularly upfield shifted and well resolved for both WT and SLIP conformations (Evans and Gardner, 2009). L391 is also a good probe to extract and compare

165 binding affinities of KG-548 and KG-655 as it is not directly involved in the binding of either compounds (and thus has minimal chemical shift changes observed in the presence of KG-548 or KG-655). We conducted the ^{13}C-^{1}H HSQC titration series with increasing concentration of KG-655 (0, 500, 1000, 2500, 5000, 10000 μM) against 250 μM concentration of ARNT PAS-B Y456T and extracted C_L and K_d as described above. For comparison, we additionally conducted a ^{13}C-^{1}H HSQC titration series for KG-548 (0, 500, 1000, 2000, 3000, 4000 μM) against 250 μM concentration of ARNT PAS-B

170 Y456T. We attempted to match the concentration of KG-548 to the concentrations used for KG-655, but was unable to exceed a maximum of 4000 μM for KG-548 without substantially increasing DMSO concentration.

3   Results

3.1   Impact of temperature and ionic strength on conformational equilibrium

To characterize the thermodynamics of the WT:SLIP conformational change, we used ^{15}N-^{1}H HSQC spectra of
175   ARNT PAS-B Y456T to calculate the populations of WT and SLIP states at temperatures between 278 K and 328 K. Below
300K, the conformational equilibrium is linearly dependent on temperature from 275 to 303 K (**Figure 2a**), with a
progressive bias towards the WT conformation with increasing temperature, suggesting that the conversion process is
endothermic. Using data 303K and below, we plotted the natural logarithm of the equilibrium constant versus the inverse of
the temperature and used the linear region of the plot to determine ΔH (6.8 kcal/mol), ΔS (23.9 cal/mol-K), and ΔG$_{298K}$ (-
180   0.31 kcal/mol) of the SLIP to WT conversion (**Figure 2b)**, confirming that it is indeed endothermic but slightly favored
overall due to entropic considerations.

Figure 2 – Temperature dependence of WT:SLIP conformational equilibrium in ARNT PAS-B Y456T. (a)
Conformational preference of ARNT PAS-B Y456T at temperatures between 278 and 323 K. The equilibrium is linearly
dependent on temperature (red line) between 278 and 303 K. Above 303 K, the equilibrium remains constant. (b) The
data from panel (a) converted to ln(K$_{eq}$) *versus* 1/T with the linear region (278-303 K) fit to a linear equation (red).

Above 300 K, we observed a levelling of the equilibrium at approximately 2:1 (WT:SLIP). We attribute this to
protein aggregation at higher temperatures, as seen by a decrease in peak intensity across the ^{15}N-^{1}H HSQC spectrum, likely
due the partial unfolding during interconversion between WT and SLIP conformations (Evans and Gardner, 2009;Xu, 2020).
185   Studies on several proteins that slowly interconvert between two different conformations, such as lymphotactin
(Tuinstra et al., 2008) and drk SH3 (Zhang and Forman-Kay, 1995), have shown that solvent conditions such as counterion
identity and ionic strength can readily shift such equilibria. Therefore, we determined whether changes in such parameters
similarly affect the equilibrium between the two folded states of ARNT PAS-B Y456T. We assessed the impact of changing
buffers and pH values (either Tris or PIPES buffers, over total range of pH 6.0 – 9.0), along with salt concentrations (50 –
190   200 mM NaCl) by using ^{15}N-^{1}H HSQC spectra to determine the relative populations the two states (**Supplementary Figure**

MAGNETIC RESONANCE
Open Access
Discussions

S1). We discovered that these effects were minimal, as no substantial (greater than a 5% deviation) changes were observed for independent pH and salt titrations. These results are consistent with the relatively similar amino acid types exposed to solvent in the two conformations of the Iβ-strand.

3.2 Impact of HI loop length and sequence on conformational equilibrium

195   We previously reported that additional mutations in the Y456T background can alter the WT:SLIP equilibrium (**Table 1, left column**). At an extreme, we could lock the protein into the SLIP conformation by adding the F444Q and F446A point mutations on the Hβ strand to the Y456T background, enabling structural characterization of the SLIP conformation (Evans et al., 2009). Another potential contributor to the WT:SLIP equilibrium is the HI loop (residues 447-454), which connects the Hβ and the Iβ strand. This loop is highly flexible in the wildtype ARNT PAS-B domain, showing

200   intermediate exchange broadening of NMR signals at several sites (Card et al., 2005). In the SLIP conformation, the HI loop shortens and packs more tightly against the domain core; as well, the N448-P449 peptide bond within the loop isomerizes from trans (WT) to cis (SLIP). We have previously shown that although the P449 residue has minor impact on the equilibrium WT:SLIP levels, this residue plays a critical role in the kinetics of interconversion (Evans et al., 2009;Evans and Gardner, 2009). To further explore the role of P449, we investigated two changes to P449 here (**Table 1, right column**).

205   First, we generated a P449A point mutant to proline to keep the 448-449 peptide bond in a *trans* configuration and provide more flexibility in the HI loop, both of which are normally associated with the WT conformation. In the ^{15}N-^{1}H HSQC spectrum of this mutant, multiple peaks were observed for each amide residue (approximately three-fold more than in wildtype), none of which overlap with SLIP peaks, **Supplementary Figure S2**. This suggests that the added flexibility by the P449A mutation destabilizes the WT conformation and allows ARNT PAS-B to sample and adopt new stable

210   conformations different from the previously-characterized SLIP state. In addition, mutating P449 to either Ala or Gly in the Y456T background shifted the WT:SLIP equilibrium from the initial 51:49 value to 32:68 or 9:91, respectively. These

Table 1: Percent WT, SLIP in different mutants ARNT PAS-B sequence variants

Mutation	% WT conformation	% SLIP conformation	Mutation	% WT conformation	% SLIP conformation
WT	>99	<1	Y456T + TEV Site Cleaved	20	80
Y456A	>98	<2	Y456T + TEV Site Uncleaved	19	81
Y456S	81	19	P449A	14	_a
Y456T	50	50	P449G/Y456T	9	91
P449A/Y456T	32	68	F444Q/F446A/ P449A/Y456T	7	93
F444Q/Y456T	19	81			
F444Q/F446A/Y456T	<1	>99			

All ratios established by ^{15}N-^{1}H HSQC spectra of each protein. Mutations listed in left shaded column have been previously published in (Evans et al., 2009). [a] Mutation P449A resulted in three additional conformations that are not the SLIP conformation, percentage breakdown of these additional conformations are 60, 14, and 12.

results suggest that the identity of the P449 residue impacts the WT:SLIP equilibrium, albeit in a role secondary to mutations in the β-sheet residues.

Having found that mutations that increased flexibility at the HI loop proline could affect the relative populations of
215 the WT and SLIP conformations, we wanted to test whether the length of the HI loop itself could contribute to the equilibrium. By integrating a TEV protease site into the middle of the HI loop (E-N-L-Y-F-Q, inserted between Y450 and S451), we could examine both how this insertion – and subsequent removal of the covalent linkage – would allow the Iβ-strand to slip while keeping the protein folded. NMR characterization of Y456T with this loop insertion showed that the equilibrium between WT and the SLIP conformation was shifted to 20:80, suggesting that the addition of six residues in the
220 HI loop favours slippage of the Iβ-strand and adopt the SLIP conformation. Notably, after cutting with TEV protease, cleaving between the newly-introduced glutamine and S451, the equilibrium between the two conformations remained unchanged. The sample was applied to a MonoQ column to separate the two conformations, as we previously demonstrated (Evans et al., 2009); immediately after injection onto the column, a precipitate formed, rendering it impossible to carry out the separation. We interpret the precipitation as arising from dissociation of the Iβ-strand peptide, as it is not observed either
225 for this construct prior to TEV protease treatment nor for the wildtype protein. These results confirm that length in the HI loop influences the conformation of the Iβ-strand.

3.3 Mutations that promote SLIP conformation also affect the denatured state of ARNT PAS-B

Since the interconversion between WT and SLIP conformations proceeds through a chiefly unfolded transition state (Evans and Gardner, 2009;Xu, 2020), we hypothesized that the structure of the denatured state of the ARNT PAS-B may
230 bias the WT:SLIP equilibrium. To address this possibility, we recorded triple-resonance NMR experiments on ARNT PAS-B wildtype, Y456T, and F444Q/F446A/Y456T in 8 M urea (a concentration at which most of the protein should be unfolded, **Supplementary Figure S3**) and used these data to assign the majority of backbone resonances for the three variants. From these data, we predicted backbone amide N-H S^2 order parameters and secondary structure propensities in the unfolded state from measured chemical shifts using TALOS+ and SSP (Shen et al., 2009;Marsh et al., 2006), respectively. The predicted
235 order parameters are consistent with all three proteins being highly flexible ensembles, with the majority of residues (85/119, 71%) displaying S^2 values < 0.6 and only 11 residues displaying S^2 values > 0.75. Consistent with this denatured state, the SSP algorithm predicted low amounts of residual secondary structure for all three proteins, with most residues populating from 0 to 25% extended structure, **Figure 3**.

The predicted order parameters are very similar for all three variants; the greatest difference is between residues 440
240 and 450 (Hβ-strand and HI loop), where the denatured F444Q/F446A/Y456T mutant (SLIP conformation) displays more order than the wildtype or Y456T proteins. In addition, the triple mutant has decreased extended structure propensity in the same region. Some of these differences may be due to the mutations present in this region; this is more likely for the secondary structure propensity, which also detects a difference between the mutated and wildtype proteins in the region
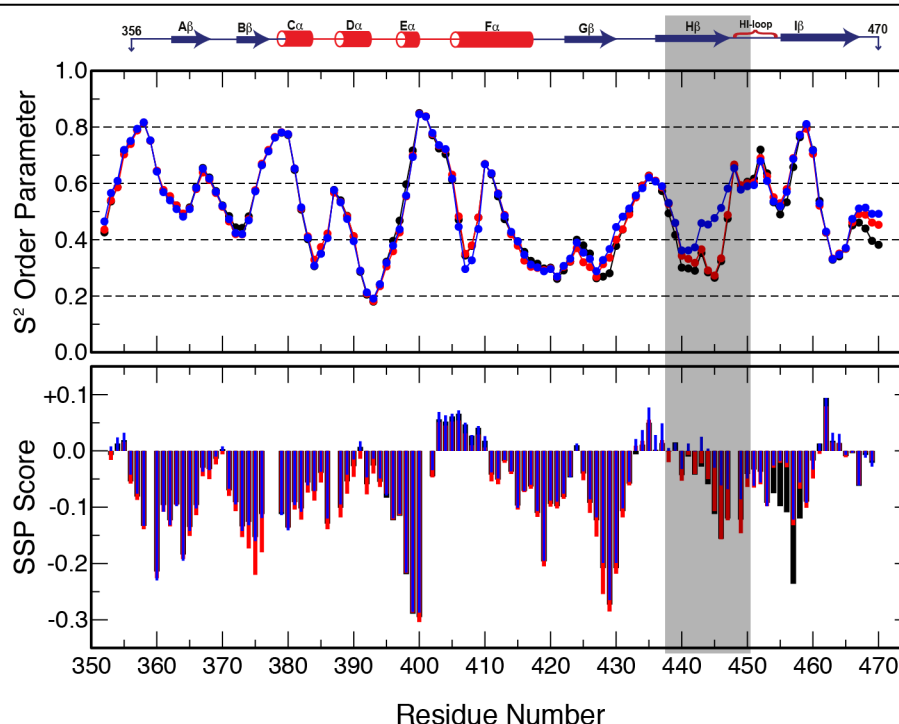
Figure 3 – Backbone flexibility and secondary structure preference of ARNT PAS-B variants under urea denaturing conditions. N-H S^2 order parameter predicted by TALOS+ (top) and residual secondary structure predicted by SSP (bottom; positive = helix, negative = strand) for ARNT PAS-B wildtype (black), Y456T (red), and F444Q/F446A/Y456T (blue) denatured in 8 M urea. The region of largest S^2 difference is shaded grey and the secondary structure elements of the folded wildtype protein are shown above the plot.

around residue 456 (also mutated). However, the S^2 values mainly differ in the Hβ-strand region, and also follow a rank order of F444Q/F446A/Y456T>Y456T>wildtype for residues 438-442. These findings show that the mutations that favor the SLIP conformation in the folded state also affect the residual structure in the unfolded state.

3.4 Compounds can bind preferentially to WT or SLIP conformations

PAS domains can bind a variety of small molecules without disrupting the overall PAS fold (Henry and Crosson, 2011). Therefore, we tested whether small, artificial ligands could preferentially bind to either the WT or SLIP conformations of ARNT PAS-B. We conducted a screen using a thermal shift assay against ARNT PAS-B wildtype (WT:SLIP, 100:0), Y456T (51:49), and F444Q/Y456T (19:81). This screen utilized a library of approximately 760 chemical fragments (MW 203 Da on average, ±73 Da s.d.) which we have previously used in NMR-based screens of a variety of targets (Amezcua et al., 2002;Best et al., 2004;Guo et al., 2013;Scheuermann et al., 2009). Using it here in a thermal screen assay, we observed that twenty-six compounds resulted in substantial T_m changes ($\Delta T_m > 4$ ºC), suggesting that they bound the WT, SLIP, or both conformations (**Figure 4**). Notably, the T_m of ARNT PAS-B decreased upon the addition of any of the twenty-six compounds, suggesting that ARNT PAS-B somehow becomes less stable when these compounds bind.
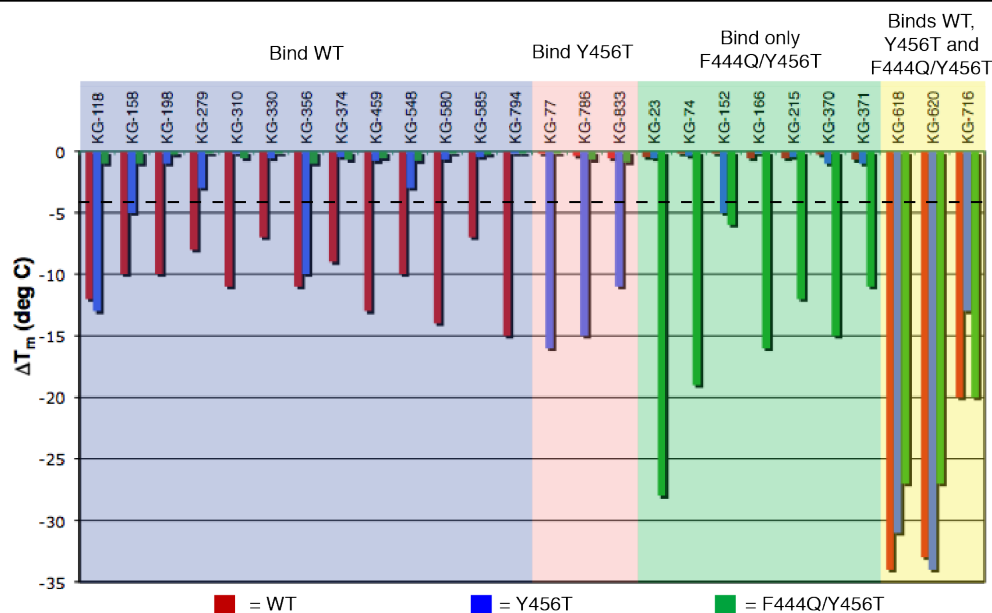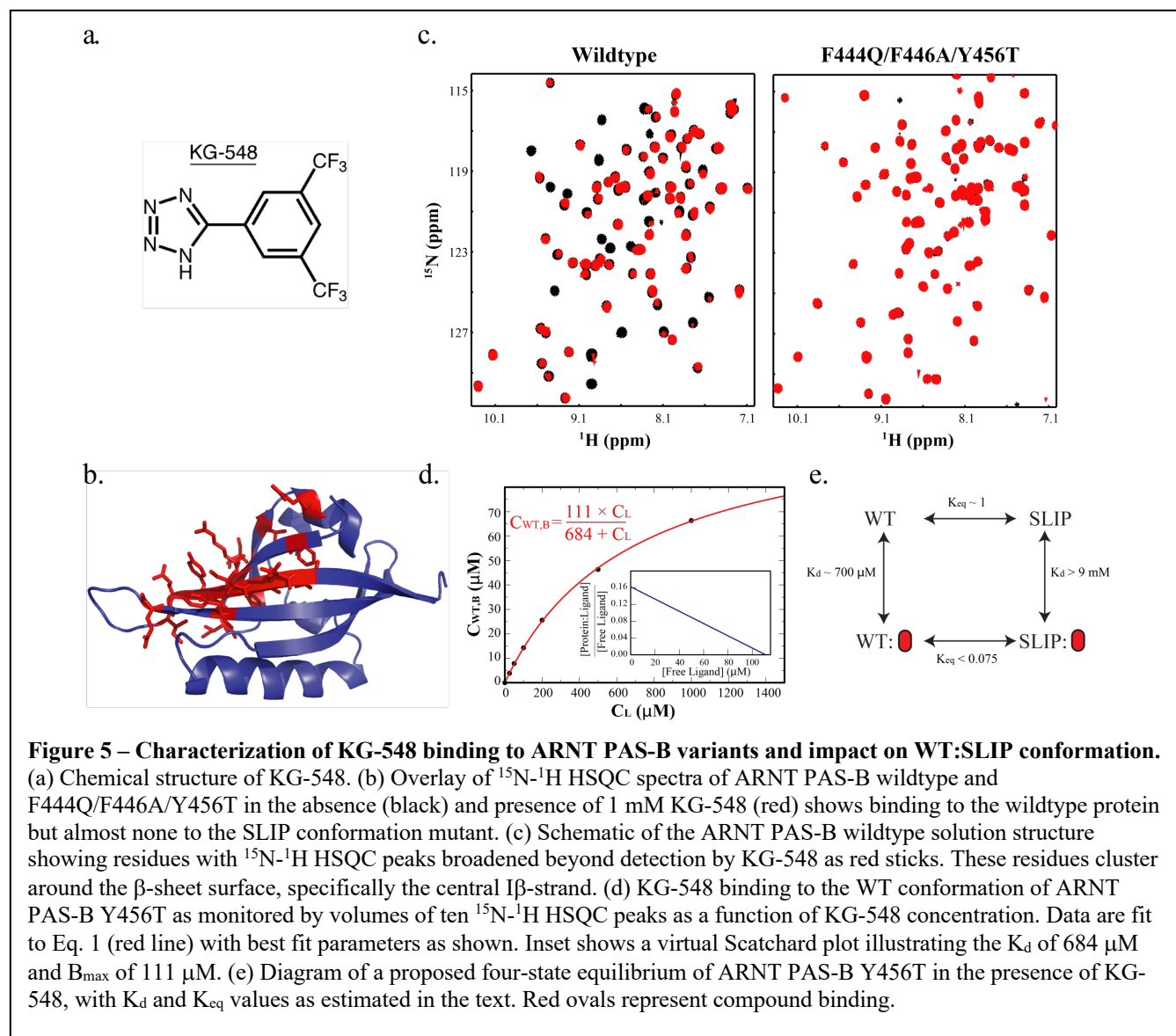
MAGNETIC
RESONANCE
Discussions
Open Access

Figure 4 – Fragment screening of ARNT PAS-B variants. Binding of small molecules to ARNT PAS-B wildtype (red), Y456T (blue), and F444Q/Y456T (green) as measured by change in T_m in the thermal shift assay, comparing T_ms recorded with and without 50 μM compound present. Only compounds that resulted in greater than 4 ºC T_m shifts are shown.

Confirmation of compound binding by NMR revealed that three of the twenty-six initial hits bound only ARNT PAS-B Y456T and not the wildtype or the double mutant proteins. These initial hits were removed from further analysis. Of the twenty-three remaining compounds, thirteen preferentially bound to the wildtype protein, seven preferentially bound to the

260   ARNT PAS-B F444Q/Y456T variant, and three bound to all ARNT PAS-B variants. Taken together, these data demonstrate that ligands could preferentially bind one conformation over the other.

We identified several lead compounds using the abovementioned approach. One of these compounds, KG-548 (5-(3,5-bis(trifluoromethyl)phenyl)tetrazole), **Figure 5a**, exhibited slow exchange behaviour, with over 30 amide sites substantially broadened in the ^{15}N-^1H HSQC spectrum, **Figure 5b, left**. The broadened peaks arise from residues that mostly

265   localize to the β-sheet, **Figure 5c**. Given this evidence that KG-548 binds the ARNT PAS-B WT conformation, we tested whether the compound could bind to the SLIP conformation by recording ^{15}N-^1H HSQC spectra of ARNT PAS-B F444Q/F446A/Y456T in the presence and absence of KG-548. Interestingly, there were no significant spectral changes for the triple mutant protein upon addition of 1 mM KG-548, thereby indicating minimal interaction with the compound at best, **Figure 5b, right**. This confirms the initial findings by thermal shift assay that compounds can have markedly different

270   binding affinities to either the WT or SLIP conformation. Intriguingly, we have also identified KG-548 in a screen for compounds that disrupt ARNT PAS-B binding to the coiled-coil coactivators TRIP230 and TACC3 (Guo et al., 2013), suggesting that its binding can affect the conformation of the β-sheet surface. More recently, through high-pressure NMR analysis, complemented by site-directed mutagenesis studies, we confirmed KG-548 to be a surface binding ligand,

interacting hydrophobically with residues I364 and I458 on the external β–sheet surface of wildtype ARNT PAS-B (Gagné,

275   2020), which would explain the preferential binding, as I458 is flipped inward to the core of the protein in the SLIP

conformation.

Figure 5 – Characterization of KG-548 binding to ARNT PAS-B variants and impact on WT:SLIP conformation.
(a) Chemical structure of KG-548. (b) Overlay of ^{15}N-^{1}H HSQC spectra of ARNT PAS-B wildtype and
F444Q/F446A/Y456T in the absence (black) and presence of 1 mM KG-548 (red) shows binding to the wildtype protein
but almost none to the SLIP conformation mutant. (c) Schematic of the ARNT PAS-B wildtype solution structure
showing residues with ^{15}N-^{1}H HSQC peaks broadened beyond detection by KG-548 as red sticks. These residues cluster
around the β-sheet surface, specifically the central Iβ-strand. (d) KG-548 binding to the WT conformation of ARNT
PAS-B Y456T as monitored by volumes of ten ^{15}N-^{1}H HSQC peaks as a function of KG-548 concentration. Data are fit
to Eq. 1 (red line) with best fit parameters as shown. Inset shows a virtual Scatchard plot illustrating the K_d of 684 μM
and B_{max} of 111 μM. (e) Diagram of a proposed four-state equilibrium of ARNT PAS-B Y456T in the presence of KG-
548, with K_d and K_{eq} values as estimated in the text. Red ovals represent compound binding.

3.5   KG-548 and KG-655 drive the conformational equilibrium towards the WT state

Since KG-548 preferentially binds the wildtype ARNT PAS-B, the addition of this compound to Y456T should

drive the 51:49 (WT:SLIP) equilibrium towards the WT conformation. We performed a titration with increasing

280   concentrations of KG-548 (0 – 1000 μM) against 200 μM ARNT PAS-B Y456T, observing a shifted equilibrium of 77:23

12

(WT:SLIP) at the highest ligand concentration. Due to the broadening of several peaks in the presence of the compound, we analyzed only those peaks that were not affected by ligand binding. Despite the difficulties posed by the broadening of peaks of interest (see Methods), we determined the binding affinity ($K_D = 684 \pm 33.1 \mu M$) and maximum binding ($B_{max} = 111 \pm 7.1$ μM, compare to ~100 μM WT conformation in 200 μM ARNT PAS-B Y456T sample) of KG-548 for the WT conformation

285 of ARNT PAS-B Y456T, **Figure 5d**.

We additionally tested the preferential binding ability of KG-655 (3,5-bis(trifluoromethyl)phenol), a fragment of KG-548 (with tetrazole replaced by a hydroxyl group), which was also shown to disrupt ARNT PAS-B binding to TACC3 (Guo et al., 2013). We previously showed that this ligand binds to two sites of wildtype ARNT PAS-B, both to the external side of the β-sheet surface and internally to the core of the domain (Gagné, 2020). We again performed titration experiments

290 with increasing concentration of KG-655 (0 – 10 mM), and expectedly saw binding specificity towards the WT conformation, similar to KG-548 (**Supplementary Figure S4a**). Due to extensive chemical shift changes and broadening of many amide peaks in the presence of KG-655, we turned to $^{13}C/^1H$-HSQC titration experiments to extract binding affinities (see Methods). We chose to monitor the upfield-shifted L391 δ1 methyl signals because these peaks were well resolved in 1D and 2D NMR spectra and have been previously used to monitor the relative population changes between the two

295 conformations (Evans and Gardner, 2009) (Xu, 2020) (**Supplementary Figure S4b**). As an initial control, we calculated the dissociation constant ($K_d = 414 \pm 7.1 \mu M$) of KG-548 using this approach, comparable to the number reported above ($K_d = 684 \pm 33.1 \mu M$). With the same method, we extracted a K_d of KG-655 ($1947 \pm 152 \mu M$) to ARNT PAS-B Y456T (**Supplementary Figure S4c**). Despite having extremely low binding affinity, the binding of KG-655 undoubtedly shifted the equilibrium towards the WT conformation. Interestingly, the surface binding of KG-655 to the WT conformation of

300 ARNT PAS-B Y456T appeared to be abolished, leaving internal binding as the only binding mode for KG-655 (**Supplementary Figure S5**). We posit this is potentially due the loss of necessary interactions between the ligand and residue Y456. Taken together, these data confirm our previous findings that compounds can preferentially bind to a specific conformation of ARNT PAS-B, and shift the equilibrium in the process. As noted above, we achieved population shifts with both surface- and core-binding ligands (KG-548 and KG-655, respectively).

305 The two examples above support a four-state model with the following states varying by conformation (WT, SLIP) and ligand binding (apo, bound), **Figure 5e**. In theory, the compound also binds the SLIP conformation, but our NMR data shows that the affinity between the two is minor, with no bound state visible even at the highest ligand concentration. Assuming that an invisible bound state would represent at most 10% of the protein in the SLIP conformation at the highest ligand concentration, we calculated a lower bound of 9 mM for the dissociation constant of KG-548 using Eq. 1, and even

310 higher for KG-655. Taking KG-548 as an example, the value calculated allows us to estimate the equilibrium constant between WT bound and SLIP bound states, as presented in **Figure 5e**. With the addition of compound to Y456T, the compound binds the WT conformation, creating a new WT bound state. This process depletes the WT unbound state, thereby driving the SLIP conformation towards WT to re-establish equilibrium.

**MAGNETIC
RESONANCE**
Discussions

4   Discussion

315   We have previously established the structural plasticity of the PAS-B domain of ARNT, which is highly sensitive to the side-chain at position 456, located in the Iβ-strand (Evans et al., 2009;Evans and Gardner, 2009;Xu, 2020). In the wildtype protein, this position is occupied by a tyrosine and the sidechain is solvent-exposed. Reducing the size of Y456 to a smaller sidechain enables ARNT PAS-B to enter an equilibrium between two stable conformations, the original WT state and a new SLIP state with a three-residue slip and inversion of the Iβ-strand which places this side-chain into the core of the

320   protein. Here we extend our prior demonstrations of the ability of nearby mutations to influence the WT:SLIP equilibrium by evaluating the impact of environmental conditions, the HI loop, and small molecule binding on this interconversion. Taken together, these features give control over this uncovered flexibility intrinsic to this PAS domain.

It is clear that many PAS domains have significant intrinsic flexibility, particularly in the β-sheet surface and the final β-hairpin, consisting of HI loop linking the Hβ- and Iβ-strands. Supporting this idea, residues in the HI loop show

325   intermediate exchange broadening in $^{15}N/^{1}H$ spectra of the wildtype ARNT PAS-B domain (Card et al., 2005), and when this domain is subjected to mechanical unfolding *in silico*, about 1/3 of the unfolding trajectories include a transient intermediate in which the C-terminal β-hairpin is unfolded (Gao et al., 2012). While this flexibility is expected to play a role in ligand binding to the core of a PAS domain, it is not evident in the static crystal structures of ligand-bound PAS domains. For example, only a few residues in the Iβ-strand of HIF-2α PAS-B show a significant (> 0.5 Å) backbone shifts between the

330   apo and ligand-bound states (though note some large changes in the AB and HI loops) (Scheuermann et al., 2015;Wu et al., 2015;Scheuermann et al., 2013). While the ARNT PAS-B mutations described here are not found naturally to the best of our knowledge, they may uncover hidden flexibility or fragility of the fold that cannot be seen in crystal or averaged solution structures.

Our studies here and elsewhere (Evans et al., 2009;Evans and Gardner, 2009;Xu, 2020) on ARNT PAS-B Y456T

335   comprise a toolkit for examining fragile protein folds and metamorphic proteins. Many of the approaches and lessons discussed here could be applicable to other similar biological systems, including some that have already been applied. For a simple example, the metamorphic protein IscU, which forms iron-sulfur clusters in *E. coli*, interconverts between two states in the process of carrying out its function; this interconversion requires *cis-trans* isomerizations of two proline peptide bonds (Dai et al., 2012). This is reminiscent of the isomerization of the P448-N449 peptide bond that accompanies the switch from

340   the WT to the SLIP conformation in ARNT PAS-B Y456T.

Critical to the ability for controlled switching between states is a small free energy difference between them. For ARNT PAS-B, we identify this as being -0.3 kcal/mol at 298 K – less than one hydrogen bond, illustrating that the loss or gain of only a few interactions would be enough to switch between the folds. The breakdown of enthalpic and entropic contributions (ΔH: +6.8 kcal/mol, ΔS: +23.9 cal/mol-K) suggests that there are actually more favourable interactions in the

345   SLIP state, but entropic considerations favour the WT state. Calculation of thermodynamic parameters of interconversion is

relatively straightforward and could provide hints to the environmental triggers that favour one state over another in metamorphic proteins.

Fragile folds may interconvert through unfolded intermediates, or proceed through series of partially structured transitions (Tyler et al., 2011;Zhao et al., 2016;Khatua et al., 2020). We previously reported that the interconversion between the WT and SLIP conformations in ARNT PAS-B Y456T goes through a mostly-unfolded intermediate that then refolds into two similarly stable folded states (Evans and Gardner, 2009;Xu, 2020). We find that the denatured state of the F444Q/F444A/Y456T mutant that favours the SLIP conformation has slightly greater order at the C-terminal end of the Hβ-strand. We posit that the Hβ-strand may form a folding core or nucleus in the F444Q/F446A/Y456T mutant that promotes folding into the SLIP conformation; rigidity of the C-terminal end of the Hβ-strand may force the Iβ-strand to slip toward the C-terminus of the protein. It is also interesting and counterintuitive that, in this case, removing phenylalanine residues results in greater order in the unfolded state, since folding cores are often made up of such hydrophobic residues (Alexandrescu and Shortle, 1994;Buck et al., 1996;Klein-Seetharaman et al., 2002).

Changes in β-strand register have been noted in well-folded proteins, albeit rarely (Eigenbrot et al., 2001;Goldberg, 1998;Tuinstra et al., 2008;Wright and Scarsdale, 1995;Volkov et al., 2016). These findings prompted *in silico* studies to investigate such phenomena, where rearrangements of β-strand register have been observed through implicit and explicit solvent molecular dynamics (MD) simulations (Panteva et al., 2011;Li et al., 2007). However, during MD simulations of β-hairpin folding, it is often difficult to establish native β-strand register (Shao et al., 2013). While this has been attributed to several causes, including force field errors (Kuhrova et al., 2012), we suggest that it may reflect an underlying biophysical phenomenon: the importance of hydrophobic clusters on the "inside" face of the hairpin. In the case of proper folding, the formation of hydrophobic clusters on one face of the sheet drives the correct alignment of the β-strands relative to each other and formation of cross-strand hydrogen bonds (Shao, 2015;Shao et al., 2013). This description may be applicable to the situation of ARNT PAS-B Y456T and F444Q/F444A/Y456T, as these two mutants progressively weaken a hydrophobic cluster (in this case found on the solvent-facing side of the β-sheet), thus allowing the Iβ-strand to slip during folding. In fact, due to the hydrated cavity within ARNT PAS-B, it is an almost "inside-out" protein, with the solvent-exposed side of the β-sheet containing 12 polar and 11 non-polar residues, and 8 polar and 12 non-polar on the other side. The C-terminal β-hairpin is the most egregious example, with the Hβ-strand containing more aromatic residues on the solvent-exposed side and more polar residues on the other side and both sides of the Iβ-strand containing approximately the same numbers of polar and non-polar residues. This unconventional arrangement of sidechains on the ARNT PAS-B domain, likely due to its internal water-filled cavities and function as a protein binding site, may be the driving force behind its fragile fold. Similar studies of the unfolded states of other fragile protein folds may yield insights as well.

Work from our lab and others has established that PAS domains that contain surface grooves and interior cavities can bind ligands that modulate their interactions with other proteins (Guo et al., 2015;Henry and Crosson, 2011;Scheuermann et al., 2009;Wu et al., 2015;Gagné, 2020). Since the C-terminal β-hairpin is immediately adjacent to the

interior cavity, we wondered if binding to a ligand could distinguish between the WT and SLIP conformations of ARNT
380 PAS-B Y456T. Remarkably, we identified both surface- and core- binding ligands that selectively bound to one
conformation over another. Two of these small molecules, KG-548 and KG-655, bind to the WT conformation with mid µM
to low mM affinities and do not appreciably bind the SLIP conformation ($K_d > 9$ mM). Intriguingly, we have also shown that
KG-548 and KG-655 binding to wildtype ARNT PAS-B can disrupt interactions with coiled-coil coactivators (Guo et al.,
2015), suggesting that the conformational flexibility under study here may be relevant for biological interactions involving
385 ARNT.

Finally, we emphasize our findings could complement other methods to manipulate conformational switches of
proteins. For example, we have shown that equilibrium of protein conformations can also be pressure-dependent, mainly
because of their volume and compressibility differences (Xu, 2020). Selective binding of ligands to one conformation over
the other can affect such parameters, and change interconversion thermodynamics and kinetics, and therefore provide
390 insights to the transition process. Other metamorphic proteins such as lymphotactin (Tuinstra et al., 2008) and IscU (Markley
et al., 2013) have been shown to bind to specific binding partners in different folds. The N11L mutant of the Arc repressor,
another engineered fragile fold, binds DNA and concomitantly drives the equilibrium to the native fold (Cordes et al., 2000).
Our approach should be effective for characterizing these ligand interactions with fragile protein folds, as long as these
proteins give rise to good NMR signals. Characterizing these interactions could help to reveal novel mechanisms for
395 regulating biological activity by switching between two distinct structures and a means of controlling such switches (Ha and
Loh, 2017).

5   Conclusions

We here characterize the thermodynamic components of a substantial change in protein conformation – a beta-
strand register shift in a variant of the ARNT PAS-B domain – and demonstrate how it can be manipulated with a mix of
400 environmental and sequence changes. Notably, we can exert control over the equilibrium using small molecule compounds
that preferentially bind one of the two states. Our findings suggest that it is possible to control the switch between the two
structures using small molecules, providing a route for application to other proteins exhibiting fragile folds.

Data availability

405 Data are available upon request.

Supplement

The Supplement contains the following information: Supplementary Figure S1 – S5.

Author contributions

MRE, XX, ID, and KHG designed experimental approach and strategy. MRE, XX, and LPM performed the experiments. ID,
410 XX, MRE, LPM, and KHG analyzed the data. XX, ID, MRE, KHG wrote the manuscript.

Competing interests

The authors declare that they have no conflict of interest.

Acknowledgements

Financial support

MAGNETIC
RESONANCE
Discussions

420 **References**

Alexander, P. A., He, Y., Chen, Y., Orban, J., and Bryan, P. N.: A minimal sequence code for switching protein structure and function, Proc. Natl. Acad. Sci. U. S. A., 106, 21149-21154, 10.1073/pnas.0906408106, 2009.

Alexandrescu, A. T., and Shortle, D.: Backbone dynamics of a highly disordered 131 residue fragment of staphylococcal nuclease, J. Mol. Biol., 242, 527-546, 1994.

425 Amezcua, C. A., Harper, S. M., Rutter, J., and Gardner, K. H.: Structure and interactions of PAS kinase N-terminal PAS domain: model for intramolecular kinase regulation, Structure, 10, 1349-1361, 10.1016/s0969-2126(02)00857-2, 2002.

Anfinsen, C. B.: Principles that Govern the Folding of Protein Chains, Science, 181, 223-230, 10.1126/science.181.4096.223, 1973.

430 Best, J. L., Amezcua, C. A., Mayr, B., Flechner, L., Murawsky, C. M., Emerson, B., Zor, T., Gardner, K. H., and Montminy, M.: Identification of small-molecule antagonists that inhibit an activator: coactivator interaction, Proc. Natl. Acad. Sci. U. S. A., 101, 17622-17627, 10.1073/pnas.0406374101, 2004.

Bisson, W. H., Koch, D. C., O'Donnell, E. F., Khalil, S. M., Kerkvliet, N. I., Tanguay, R. L., Abagyan, R., and Kolluri, S. K.: Modeling of the aryl hydrocarbon receptor (AhR) ligand binding domain and its utility in virtual ligand screening to 435 predict new AhR ligands, J. Med. Chem., 52, 5635-5641, 10.1021/jm900199u, 2009.

Buck, M., Schwalbe, H., and Dobson, C. M.: Main-chain dynamics of a partially folded protein: 15N NMR relaxation measurements of hen egg white lysozyme denatured in trifluoroethanol, J. Mol. Biol., 257, 669-683, 10.1006/jmbi.1996.0193, 1996.

Card, P. B., Erbel, P. J. A., and Gardner, K. H.: Structural basis of ARNT PAS-B dimerization: use of a common beta-sheet 440 interface for hetero- and homodimerization, J. Mol. Biol., 353, 664-677, 10.1016/j.jmb.2005.08.043, 2005.

Cardoso, R., Love, R., Nilsson, C. L., Bergqvist, S., Nowlin, D., Yan, J., Liu, K. K.-C., Zhu, J., Chen, P., Deng, Y.-L., Dyson, H. J., Greig, M. J., and Brooun, A.: Identification of Cys255 in HIF-1α as a novel site for development of covalent inhibitors of HIF-1α/ARNT PasB domain protein–protein interaction, Protein Sci., 21, 1885-1896, 10.1002/pro.2172, 2012.

MAGNETIC
RESONANCE
Discussions
Open Access

445   Chapman-Smith, A., Lutwyche, J. K., and Whitelaw, M. L.: Contribution of the Per/Arnt/Sim (PAS) domains to DNA binding by the basic helix-loop-helix PAS transcriptional regulators, J Biol Chem, 279, 5353-5362, 10.1074/jbc.M310041200, 2004.

Cordes, M. H., Burton, R. E., Walsh, N. P., McKnight, C. J., and Sauer, R. T.: An evolutionary bridge to a new protein fold, Nat. Struct. Biol., 7, 1129-1132, 10.1038/81985, 2000.

450   Dai, Z., Tonelli, M., and Markley, J. L.: Metamorphic protein IscU changes conformation by cis-trans isomerizations of two peptidyl-prolyl peptide bonds, Biochemistry, 51, 9595-9602, 10.1021/bi301413y, 2012.

Delaglio, F., Grzesiek, S., Vuister, G. W., Zhu, G., Pfeifer, J., and Bax, A.: NMRPipe: a multidimensional spectral processing system based on UNIX pipes, J. Biomol. NMR, 6, 277-293, 1995.

Dyson, H. J.: Making Sense of Intrinsically Disordered Proteins, Biophys. J., 110, 1013-1016, 10.1016/j.bpj.2016.01.030,
455   2016.

Eigenbrot, C., Kirchhofer, D., Dennis, M. S., Santell, L., Lazarus, R. A., Stamos, J., and Ultsch, M. H.: The factor VII zymogen structure reveals reregistration of beta strands during activation, Structure, 9, 627-636, 2001.

Erbel, P. J. A., Card, P. B., Karakuzu, O., Bruick, R. K., and Gardner, K. H.: Structural basis for PAS domain heterodimerization in the basic helix--loop--helix-PAS transcription factor hypoxia-inducible factor, Proc. Natl.
460   Acad. Sci. U. S. A., 100, 15504-15509, 10.1073/pnas.2533374100, 2003.

Evans, M. R., Card, P. B., and Gardner, K. H.: ARNT PAS-B has a fragile native state structure with an alternative beta-sheet register nearby in sequence space, Proc. Natl. Acad. Sci. U. S. A., 106, 2617-2622, 10.1073/pnas.0808270106, 2009.

Evans, M. R., and Gardner, K. H.: Slow transition between two beta-strand registers is dictated by protein unfolding, J. Am. Chem. Soc., 131, 11306-11307, 10.1021/ja9048338, 2009.

465   Gagné, D. A., R.; Edupuganti, U.R.; Williams, J.; Aramini, J.M.; Akasaka, K., Gardner, K.H.: Use of high pressure NMR spectroscopy to rapidly identify internal ligand-binding voids in proteins, Manuscript under review. , preprint at bioRxiv, https://doi.org/10.1101/2020.08.25.267195, 2020.

Gao, X., Qin, M., Yin, P., Liang, J., Wang, J., Cao, Y., and Wang, W.: Single-Molecule Experiments Reveal the Flexibility of a Per-ARNT-Sim Domain and the Kinetic Partitioning in the Unfolding Pathway under Force, Biophys. J., 102, 2149-
470   2157, 10.1016/j.bpj.2012.03.042, 2012.

Gerstein, M., and Echols, N.: Exploring the range of protein flexibility, from a structural proteomics perspective, Curr. Opin. Chem. Biol., 8, 14-19, 10.1016/j.cbpa.2003.12.006, 2004.

Goldberg, J.: Structural basis for activation of ARF GTPase: mechanisms of guanine nucleotide exchange and GTP-myristoyl switching, Cell, 95, 237-248, 1998.

475 Guo, Y., Partch, C. L., Key, J., Card, P. B., Pashkov, V., Patel, A., Bruick, R. K., Wurdak, H., and Gardner, K. H.: Regulating the ARNT/TACC3 axis: multiple approaches to manipulating protein/protein interactions with small molecules, ACS Chem. Biol., 8, 626-635, 10.1021/cb300604u, 2013.

Guo, Y., Scheuermann, T. H., Partch, C. L., Tomchick, D. R., and Gardner, K. H.: Coiled-coil coactivators play a structural role mediating interactions in hypoxia-inducible factor heterodimerization, J. Biol. Chem., 290, 7707-7721,
480   10.1074/jbc.M114.632786, 2015.

Ha, J. H., and Loh, S. N.: Protein conformational switches: from nature to design, Chemistry (Easton), 18, 7984-7999, 10.1002/chem.201200348, 2012.

Ha, J. H., and Loh, S. N.: Construction of Allosteric Protein Switches by Alternate Frame Folding and Intermolecular Fragment Exchange, Methods Mol. Biol., 1596, 27-41, 10.1007/978-1-4939-6940-1_2, 2017.

485 Harper, S. M., Neil, L. C., and Gardner, K. H.: Structural Basis of a Phototropin Light Switch, Science, 301, 1541-1544, 10.1126/science.1086810, 2003.

Henry, J. T., and Crosson, S.: Ligand-binding PAS domains in a genomic, cellular, and structural context, Annu. Rev. Microbiol., 65, 261-286, 10.1146/annurev-micro-121809-151631, 2011.

Huang, N., Chelliah, Y., Shan, Y., Taylor, C. A., Yoo, S.-H., Partch, C., Green, C. B., Zhang, H., and Takahashi, J. S.: Crystal
490   structure of the heterodimeric CLOCK:BMAL1 transcriptional activator complex, Science (New York, N.Y.), 337, 189-194, 10.1126/science.1222804, 2012.

Johnson, B. A., and Blevins, R. A.: NMR View: A computer program for the visualization and analysis of NMR data, J. Biomol. NMR, 4, 603-614, 10.1007/bf00404272, 1994.

Johnson, B. A.: From Raw Data to Protein Backbone Chemical Shifts Using NMRFx Processing and NMRViewJ Analysis,
495   Methods Mol. Biol., 1688, 257-310, 10.1007/978-1-4939-7386-6_13, 2018.

Khatua, P., Ray, A. J., and Hansmann, U. H. E.: Bifurcated Hydrogen Bonds and the Fold Switching of Lymphotactin, J. Phys. Chem. B, 124, 6555-6564, 10.1021/acs.jpcb.0c04565, 2020.

Klein-Seetharaman, J., Oikawa, M., Grimshaw, S. B., Wirmer, J., Duchardt, E., Ueda, T., Imoto, T., Smith, L. J., Dobson, C. M., and Schwalbe, H.: Long-range interactions within a nonnative protein, Science, 295, 1719-1722,
500   10.1126/science.1067680, 2002.

Kuhrova, P., De Simone, A., Otyepka, M., and Best, R. B.: Force-field dependence of chignolin folding and misfolding: comparison with experiment and redesign, Biophys. J., 102, 1897-1906, 10.1016/j.bpj.2012.03.024, 2012.

Kuloğlu, E. S., McCaslin, D. R., Markley, J. L., and Volkman, B. F.: Structural rearrangement of human lymphotactin, a C chemokine, under physiological solution conditions, J. Biol. Chem., 277, 17863-17870, 10.1074/jbc.M200402200,
505   2002.

Labrecque, M. P., Prefontaine, G. G., and Beischlag, T. V.: The aryl hydrocarbon receptor nuclear translocator (ARNT) family of proteins: transcriptional modifiers with multi-functional protein interfaces, Curr. Mol. Med., 13, 1047-1065, 2013.

Li, D. W., Han, L., and Huo, S.: Structural and pathway complexity of beta-strand reorganization within aggregates of human transthyretin(105-115) peptide, J. Phys. Chem. B, 111, 5425-5433, 10.1021/jp0703051, 2007.

510 Markley, J. L., Kim, J. H., Dai, Z., Bothe, J. R., Cai, K., Frederick, R. O., and Tonelli, M.: Metamorphic protein IscU alternates conformations in the course of its role as the scaffold protein for iron-sulfur cluster biosynthesis and delivery, FEBS Lett., 587, 1172-1179, 10.1016/j.febslet.2013.01.003, 2013.

Marsh, J. A., Singh, V. K., Jia, Z., and Forman-Kay, J. D.: Sensitivity of secondary structure propensities to sequence differences between alpha- and gamma-synuclein: implications for fibrillation, Protein Sci., 15, 2795-2804,
515   10.1110/ps.062465306, 2006.

Murzin, A. G.: Metamorphic Proteins, Science, 320, 1725-1726, 10.1126/science.1158868, 2008.

Nash, A. I., McNulty, R., Shillito, M. E., Swartz, T. E., Bogomolni, R. A., Luecke, H., and Gardner, K. H.: Structural basis of photosensitivity in a bacterial light-oxygen-voltage/helix-turn-helix (LOV-HTH) DNA-binding protein, Proc. Natl. Acad. Sci. U. S. A., 108, 9449-9454, 10.1073/pnas.1100262108, 2011.

520   Norris, M., Fetler, B., Marchant, J., and Johnson, B. A.: NMRFx Processor: a cross-platform NMR data processing program, J. Biomol. NMR, 65, 205-216, 10.1007/s10858-016-0049-6, 2016.

Panteva, M. T., Salari, R., Bhattacharjee, M., and Chong, L. T.: Direct observations of shifts in the beta-sheet register of a protein-peptide complex using explicit solvent simulations, Biophys. J., 100, L50-52, 10.1016/j.bpj.2011.03.035, 2011.

525   Pantoliano, M. W., Petrella, E. C., Kwasnoski, J. D., Lobanov, V. S., Myslik, J., Graf, E., Carver, T., Asel, E., Springer, B. A., Lane, P., and Salemme, F. R.: High-density miniaturized thermal shift assays as a general strategy for drug discovery, Journal of Biomolecular Screening, 6, 429-440, 10.1089/108705701753364922, 2001.

Rivera-Cancel, G., Ko, W.-h., Tomchick, D. R., Corrêa, F., and Gardner, K. H.: Full-length structure of a monomeric histidine kinase reveals basis for sensory regulation, Proc. Natl. Acad. Sci. U. S. A., 111, 17839-17844,
530   10.1073/pnas.1413983111, 2014.

Scheuermann, T. H., Tomchick, D. R., Machius, M., Guo, Y., Bruick, R. K., and Gardner, K. H.: Artificial ligand binding within the HIF2alpha PAS-B domain of the HIF2 transcription factor, Proc. Natl. Acad. Sci. U. S. A., 106, 450-455, 10.1073/pnas.0808092106, 2009.

Scheuermann, T. H., Li, Q., Ma, H. W., Key, J., Zhang, L., Chen, R., Garcia, J. A., Naidoo, J., Longgood, J., Frantz, D. E.,
535   Tambar, U. K., Gardner, K. H., and Bruick, R. K.: Allosteric inhibition of hypoxia inducible factor-2 with small molecules, Nat. Chem. Biol., 9, 271-276, 10.1038/nchembio.1185, 2013.

Scheuermann, T. H., Stroud, D., Sleet, C. E., Bayeh, L., Shokri, C., Wang, H., Caldwell, C. G., Longgood, J., MacMillan, J. B., Bruick, R. K., Gardner, K. H., and Tambar, U. K.: Isoform-Selective and Stereoselective Inhibition of Hypoxia Inducible Factor-2, J. Med. Chem., 58, 5930-5941, 10.1021/acs.jmedchem.5b00529, 2015.

540   Shao, Q., Wang, J., Shi, J., and Zhu, W.: The universality of beta-hairpin misfolding indicated by molecular dynamics simulations, J. Chem. Phys., 139, 165103, 10.1063/1.4826461, 2013.

Shao, Q.: Folding or misfolding: the choice of beta-hairpin, J. Phys. Chem. B, 119, 3893-3900, 10.1021/jp5100654, 2015.

Sheffield, P., Garrard, S., and Derewenda, Z.: Overcoming expression and purification problems of RhoGDI using a family of "parallel" expression vectors, Protein Expr. Purif., 15, 34-39, 10.1006/prep.1998.1003, 1999.

545   Shen, Y., Delaglio, F., Cornilescu, G., and Bax, A.: TALOS+: a hybrid method for predicting protein backbone torsion angles from NMR chemical shifts, J. Biomol. NMR, 44, 213-223, 10.1007/s10858-009-9333-z, 2009.

Tuinstra, R. L., Peterson, F. C., Kutlesa, S., Elgin, E. S., Kron, M. A., and Volkman, B. F.: Interconversion between two unrelated protein folds in the lymphotactin native state, Proc. Natl. Acad. Sci. U. S. A., 105, 5057-5062, 10.1073/pnas.0709518105, 2008.

550   Tyler, R. C., Murray, N. J., Peterson, F. C., and Volkman, B. F.: Native-state interconversion of a metamorphic protein requires global unfolding, Biochemistry, 50, 7077-7079, 10.1021/bi200750k, 2011.

Volkov, O. A., Kinch, L., Ariagno, C., Deng, X., Zhong, S., Grishin, N., Tomchick, D. R., Chen, Z., and Phillips, M. A.: Relief of autoinhibition by conformational switch explains enzyme activation by a catalytically dead paralog, Elife, 5, 10.7554/eLife.20198, 2016.

555   Wright, H. T., and Scarsdale, J. N.: Structural basis for serpin inhibitor activity, Proteins, 22, 210-225, 10.1002/prot.340220303, 1995.

Wu, D., Potluri, N., Lu, J., Kim, Y., and Rastinejad, F.: Structural integration in hypoxia-inducible factors, Nature, 524, 303-308, 10.1038/nature14883, 2015.

Wu, D., Su, X., Lu, J., Li, S., Hood, B. L., Vasile, S., Potluri, N., Diao, X., Kim, Y., Khorasanizadeh, S., and Rastinejad, F.:
560   Bidirectional modulation of HIF-2 activity through chemical ligands, Nat. Chem. Biol., 15, 367-376, 10.1038/s41589-019-0234-5, 2019.

Xu, X., Gagné, D. A., Aramini, J.M., Gardner, K.H.: Volume and Compressibility Differences Between Protein Conformations Revealed by High-Pressure NMR, Biophys. J., in press, preprint at bioRxiv, https://doi.org/10.1101/2020.07.29.227322, 2020.

565   Yadid, I., Kirshenbaum, N., Sharon, M., Dym, O., and Tawfik, D. S.: Metamorphic proteins mediate evolutionary transitions of structure, Proc. Natl. Acad. Sci. U. S. A., 107, 7287-7292, 10.1073/pnas.0912616107, 2010.

Zhang, O., and Forman-Kay, J. D.: Structural characterization of folded and unfolded states of an SH3 domain in equilibrium in aqueous buffer, Biochemistry, 34, 6784-6794, 1995.

Zhao, Y., Li, L., Wu, C., Jiang, X., Ge, B., Ren, H., and Huang, F.: Stable folding intermediates prevent fast interconversion between the closed and open states of Mad2 through its denatured state, Protein Eng. Des. Sel., 29, 23-29, 10.1093/protein/gzv056, 2016.

570